Polar Science 15 (2018) 55–61

Contents lists available at ScienceDirect

Polar Science

journal homepage: www.elsevier.com/locate/polar

Vertical distribution of the sound-scattering layer in the Amundsen Sea, Antarctica

Hyungbeen Lee[a], Hyoung Sul La[b,*], Donhyug Kang[c], SangHoon Lee[b]

[a] West Sea Fisheries Research Institute, Republic of Korea
[b] Korea Polar Research Institute, Republic of Korea
[c] Korea Institute Ocean Science and Technology, Republic of Korea

ARTICLE INFO

Keywords:
Sound-scattering layer (SSL)
Acoustic backscatter
Weighted mean depth (WMD)
Mixed layer depth
Amundsen Sea

ABSTRACT

Mid-trophic level at high-latitude coastal water in the Southern Ocean reside unique geographical condition with sea ice, coastal polynya, and ice shelf. To investigate the regional differences in their vertical distribution during summer, we examined acoustic backscatter data from scientific echo sounder, collected in the three representative regions in the Amundsen Sea: pack ice zone, coastal polynya zone, and ice shelf zone. The weighted mean depths (WMDs) representing zooplankton were calculated with the high resolution acoustic backscatter (1-m depth) to identify the vertical variability of the sound-scattering layer (SSL). WMDs were mainly distributed between 50 and 130 m exhibiting clear regional differences. The WMDs were detected in the shallow depth ranged between 48 and 84 m within the pack ice and coastal polynya, whereas they were observed at deeper depths around near ice shelf ranged between 117 and 126 m. WMDs varied with changing the stratification of water column structure representing strong linear relationship with the mixed layer depth ($r = 0.69$). This finding implies that understanding the essential forcing of zooplankton behavior will improve our ability to assess the coastal ecosystem in the Southern Ocean facing dramatic change.

1. Introduction

The Amundsen Sea has received much attention recently as the most rapidly changing part of the cryosphere (Smith et al., 2011), with massive ice mass loss by heat transfer beneath the ice shelves from warm water intrusion (Jenkins et al., 2010; Jacobs et al., 2011), ice-sheet surface warming (Schneider et al., 2012), and significant decline in sea ice cover (Turner et al., 2009). These physical changes are likely to affect the ecosystem in the Amundsen Sea.

Zooplankton play a major role in the ecosystem; they consume a major proportion of primary producers, and form the principal food source for a large number of high-trophic level species (Ross et al., 2008; Swadling et al., 2010). To understand the zooplanktonic ecosystem in the Southern Ocean, it is essential to observe their vertical distribution, and how their main depths are controlled by environmental conditions. The vertical distribution is a basic behavior of zooplankton associated with diel vertical migration, swarming, and feeding (Hamner et al., 1983; Ambler and Miller, 1987; Cornet and Gili, 1993; Saito and Hattori, 1997). Zooplankton distribution is significantly affected by primary productivity, temperature, seasonal and interannual sea ice cover, and environmental variability (Atkinson, 1998; Bathmann et al., 2000; Pinkerton et al., 2010). Lee et al. (2013) and Wilson et al. (2015) have described mesozooplankton communities and their grazing impact in the Amundsen Sea during the early austral summer. La et al. (2015) showed the spatial and temporal variability of *Euphausia crystallorophias* (ice krill) using acoustic methods.

Despite the ecological significance of the zooplankton ecosystem, few studies have been conducted in the Amundsen Sea coastal polynya, as the harsh weather and sea ice limits access to areas suitable for *in-situ* observations (Lee et al., 2013; La et al., 2015; Wilson et al., 2015). Moreover, the relationship between vertical variability of zooplankton and the accompanying different water column structures in the coastal polynyas remains poorly understood.

We conducted acoustic surveys to address vertical distributions of the sound-scattering layer (SSL), a concentrated layer of marine organisms such as zooplankton and nekton, in the Amundsen Sea. Acoustic systems have been used throughout the Southern Ocean to investigate the distribution, stock estimates, and ecology of krill (Brierley et al., 2006; CCAMLR, 2010; Fielding et al., 2012; La et al., 2015). It is an appropriate method of assessing the fine-scale vertical variation of the SSL.

During summer, the Amundsen Sea is generally distinguished by

* Corresponding author. Korea Polar Research Institute, Incheon 21990, Republic of Korea.
E-mail address: hsla@kopri.re.kr (H.S. La).

https://doi.org/10.1016/j.polar.2017.12.003
Received 14 September 2017; Received in revised form 2 November 2017; Accepted 18 December 2017
Available online 19 December 2017

three subzones related to the seasonal variation in sea ice: the pack ice zone, the coastal polynya zone, and the near ice shelf zone. Thus, the Amundsen Sea is an ideal location for examining the vertical distribution response of the SSL related to different hydrological features. We describe the main depth of the SSL in the different designated regions. In the Amundsen Sea, with its abundant macro- and microzooplankton (Wilson et al., 2015), primary production has been suggested as the main factor controlling zooplankton abundance (Lee et al., 2013; Wilson et al., 2015). The mixed layer depth (MLD) affects light and nutrient availability for phytoplankton, and thus affects production at the base of the pelagic food web (Diehl et al., 2002; Sebastian et al., 2012). Thus, we compared the acoustic results with the MLD, which is one of the primary factors affecting the vertical habitats of zooplankton.

2. Materials and method

2.1. Survey area

The study was conducted in the Amundsen Sea during the austral summer of 2011 on the IBRV *Araon*. For the purpose of characterizing spatial differences, the study area was divided into three regional segments based on the geographic location (Fig. 1): (1) the pack ice zone, (2) the coastal polynya zone, and (3) the near ice shelf zone. The three regions of acoustic transects were performed in 425.4 km (Table 1). Hydrographic measurements were undertaken at stations along each transect (Fig. 1, Table 2).

2.2. Hydrographic data and net sample data

Vertical profiles of seawater potential temperature, salinity, water pressure, and dissolved oxygen (DO) were obtained using a conductivity-temperature-depth CTD Rosette system (SeaBird Electronics, SBE-911 +) at each station (Fig. 1). The temperature and salinity profiles obtained by the CTD observations were used to calculate the sound speed and absorption coefficients from the echosounder. All data were averaged at 1 m depth intervals to eliminate undesirable noise. A difference criterion was applied to estimate the MLD from the density stratification. The MLD was defined as the depth at which the calculated *in-situ* density increased vertically by $\Delta\sigma_\theta = 0.03\,\mathrm{kg{\cdot}m^{-3}}$ more than the 10 m depth density (Schneider and Müller, 1990). A fluorometer (TD-700, Turner Design Co.) mounted on the CTD frame was

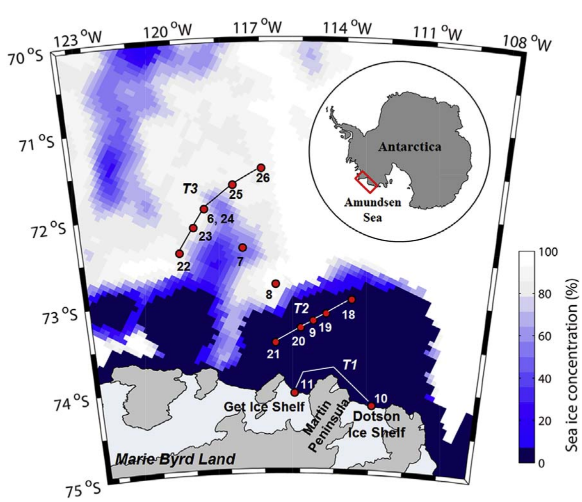

Fig. 1. Study area showing the acoustic transects (black and white line), and CTD stations (red circles) during January 2011. T1, T2, and T3 indicate the acoustic transects in the near ice shelf zone, the coastal polynya zone, and the pack ice zone, respectively. The sea ice concentration was derived from Special Sensor Microwave Imager (SSM/I) data during January 1–6, 2011. (For interpretation of the references to colour in this figure legend, the reader is referred to the Web version of this article.)

Table 1
Details for each acoustic transect survey in 2011.

Transect	Transect start time (YYYY/MM/DD, UTC)	Transect end time (YYYY/MM/DD, UTC)	Distance (km)	Geographical feature
T1	2011/01/01, 23:39	2011/01/02, 06:47	145.0	the ice shelf zone
T2	2011/01/05, 18:10	2011/01/06, 06:28	110.5	the coastal polynya zone
T3	2011/01/06, 20:03	2011/01/07, 23:55	189.9	the pack ice zone

used for the measurement of Chlorophyll *a* (Chl *a*, μg L^{-1}). The Chl *a* value obtained from the fluorometer was calibrated with measurements of Chl *a* from seawater samples collected using a Niskin-bottle attached to the CTD Rosette frame.

2.3. Acoustic data collection and analysis

Volume backscattering strength (S_v, dB re 1 m^{-1}) was collected using a Simrad EK60 scientific echosounder with a 38- and 120-kHz split-beam transducer, which was mounted onto the bottom of the ship. The hull depth of the ship was approximately 7.5 m. The 120-kHz transducer was calibrated in the survey region (117.167 °W, 71.500 °S) on January 9, 2011, following the standard procedures (Foote et al., 1987). The 38-kHz transducer wasn't calibrated due to harsh weather conditions. A pulse length of 1 ms and a ping rate of 2–5 s were employed at all frequencies, with a constant ship speed of 6 kn between sampling stations.

Acoustic data were processed using Myriax Echoview software (ver. 6.1). The S_v data were filtered to remove non-biological signals, such as surface bubbles, sea bottom, false bottom echoes, and ice breaking noise, which were identified and manually excluded. The background noise was removed using a time-varied threshold (TVT) function, as originally conceptualized by Watkins and Brierley (1996). The TVT function was applied to every ping for S_v values, and then the data were averaged at a vertical resolution of 1 m and a horizontal resolution of 185.2 m (0.1 n·mi). The noise-filtered averaged echograms between 20 and 200 m were exported from Echoview and imported into Matlab® to manipulate further treatment. The S_v above −90 dB were selected to demonstrate the vertical distribution of SSL, while S_v from small zooplankton like copepods can be removed. To compare with environmental data, S_v were averaged with 926 m (0.5 n·mi) horizontal distance before and after each station for the comparison of the environmental data.

The 120 kHz S_v, above a −90 dB integration threshold, was imported into Matlab® for further analysis to demonstrate the vertical distribution of the SSL. For analysis the weighted mean depth (WMD) was calculated to the main depth of the SSL for each station to observe the vertical variability of the SSL in the echogram (Solberg et al., 2015).

$$\mathrm{WMD} = \Sigma\,(s_v\,d_i)\,/\,\Sigma\,s_{vi},$$

where s_v and d_i are the volume backscattering strength coefficient (linear values of S_v) and its corresponding depth, respectively. Migration amplitudes were calculated as the difference in WMD between paired day and night observations.

2.4. Statistical analysis

Bivariate Pearson correlation analyses were performed to examine the relationship between the WMD and mean S_v from 20 to 200 m and environmental variables: mean temperature (°C) and salinity (psu) from surface to 200 m, mean mixed layer temperature and salinity from surface to mixed layer depth, and the maximum Chl *a* concentration (μg·l^{-1}). Mann-Whitney U test to verify the differences in mean S_v and

Table 2
Sampling station details including start date and time, and maximum water depth. IS: the near ice shelf zone, CP: the coastal polynya zone, PI: the pack ice zone.

Station	Region	Date (DD/MM/YYYY)	Start time (UTC)	End time (UTC)	Latitude (°S)	Longitude (°W)	Depth (m)
6	IS	12/30/2010	21:27	23:39	71.952	119.125	1520
7	IS	12/31/2010	06:47	12:06	72.415	117.690	530
8	IS	12/31/2010	17:55	22:20	72.833	116.480	630
9	CP	01/01/2010	03:10	08:04	73.250	115.000	830
10	IS	01/01/2011	17:14	18:08	74.207	112.497	1040
11	IS	01/01/2011	07:00	10:00	74.080	115.725	1060
18	CP	01/05/2011	17:15	18:10	73.000	113.500	435
19	CP	01/05/2011	21:29	22:20	73.167	114.500	714
20	CP	01/06/2011	01:50	03:05	73.333	115.499	845
21	CP	01/06/2011	06:28	08:09	73.500	116.500	376
22	PI	01/06/2011	19:20	20:03	72.447	120.142	1353
23	PI	01/07/2011	02:17	03:55	72.165	119.566	1300
24	PI	01/07/2011	07:45	10:00	71.952	119.125	1446
25	PI	01/07/2011	14:50	16:51	71.689	118.029	1241
26	PI	01/07/2011	21:55	23:55	71.498	116.988	1307

WMD between day and night.

Multivariate analyses were performed to verify the regional differences in environmental variables between habitats (the pack ice zone, the coastal polynya zone, and the near ice shelf zone) using the PRIMER v7 package (Clarke and Gorley, 2006) and PERMANOVA + for PRIMER (Anderson et al., 2008). The detail process for environmental variables (potential temperature, salinity, depth, Chl *a*, dissolved oxygen, nitrate and nitrite nitrogen (NO_2+NO_3), phosphate (PO_4), silicate (SiO_2), and ammonium nitrogen (NH_4)) were summarized in Jiang et al. (2014). The regional differences in environmental variables were calculated using the submodule canonical analysis of principal coordinates (CAP) of PERMANOVA+ with Euclidean distance from the log-transformed environmental data. A PERMANOVA test was conducted to verify the regional differences in the three habitats.

3. Results and discussion

3.1. Hydrographic condition and regional differences

The vertical structure of temperature and salinity clearly represents the different water column properties along the Dotson Trough, from the pack ice zone to the near Getz Ice shelf (Fig. 2). The MLD was gradually deeper from offshore to inshore, and the SIC also steeply decreased. Water temperature from the surface to 200 m ranged from −0.41 to −1.86 °C in the survey transects. From St. 6 to St. 8 in the pack ice zone, vertical temperature was almost the same, ranging from −1.27 to −1.86 °C to was relatively cold in the vertical section. At St. 9 and St. 10, the mixed layer was thick and the temperature was relatively warmer than −1.0 °C above 70 m between the coastal polynya zone and the near ice shelf zone, and the MLD became deeper, ranging from 15 to 89 m toward the ice shelf. In general, melting sea ice introduces fresh water at the surface, which stabilizes the water column and creates a well-lit shallow mixed layer.

The discrimination among 57 samples from three regional differences was plotted by a CAP using Euclidean distance from log-transformed environmental data (Fig. 3). The regional difference was clear; the stations were separated into three groups designated the pack ice zone, the coastal polynya zone, and the near ice shelf zone. The result indicated that the first squared canonical correlation was large, at $\delta^2 = 0.82$. The first canonical axis separated the stations in the pack ice zone (on the right of the plot) from stations in the coastal polynya zone and the near ice shelf zone. The second canonical axis also showed a large eigenvalue ($\delta^2 = 0.49$), discriminating the stations in the coastal polynya zone (upper left) from the stations in the pack ice zone and the near ice shelf zone. A PERMANOVA test determined the significant effects of the three habitats (pseudo-F = 15.017, $P = .001$), and pairwise comparisons in the PERMANOVA test showed the clear evidence against the null hypothesis, suggesting that three habitats are different from one another ($P < .05$) (Table 3). This result emphasizes that the environmental conditions among the three habitats are significantly different from each other, showing the unique regional specifications in the Amundsen Sea.

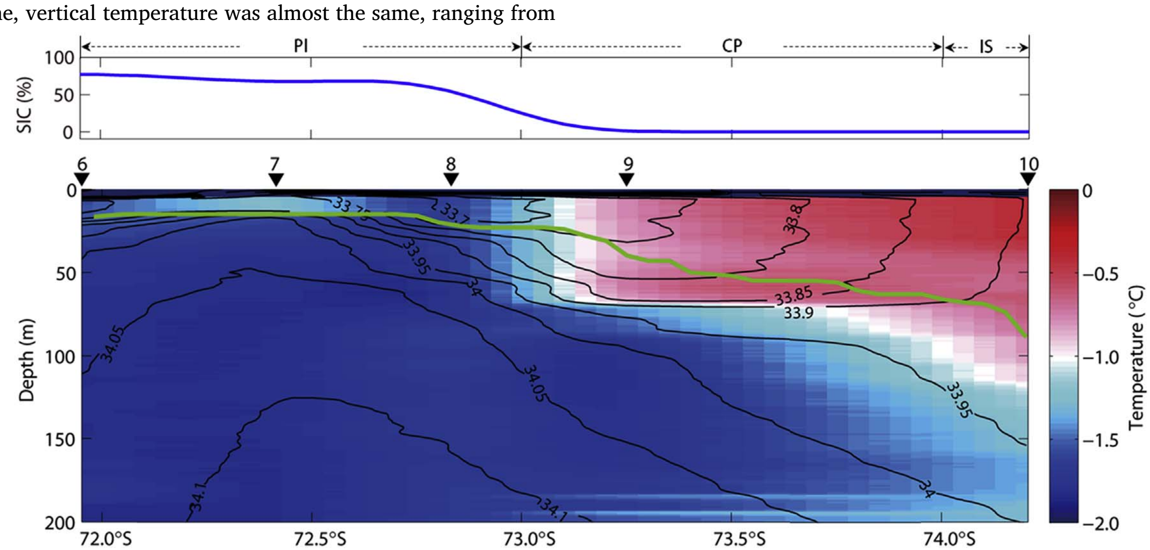

Fig. 2. Vertical section of potential temperature and salinity. Green line is the mixed layer depth. IS: the near ice shelf zone, CP: the coastal polynya zone, PI: the pack ice zone. (For interpretation of the references to colour in this figure legend, the reader is referred to the Web version of this article.)

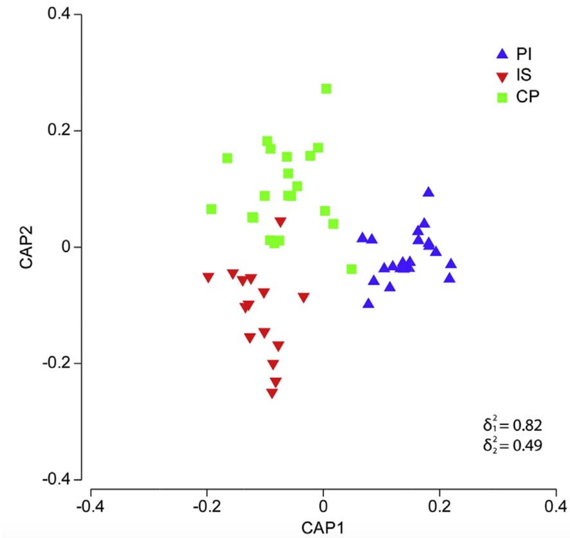

Fig. 3. Canonical analysis of principal coordinates (CAP) on Euclidean distance from log-transformed environmental variables of 57 samples from three habitats. IS: the near ice shelf zone, CP: the coastal polynya zone, PI: the pack ice zone.

3.2. Spatial distribution of sound-scattering layer

The acoustic data collected along the three transects show the different horizontal and vertical patterns of the SSL (Fig. 4). The SSL with S_v values between −90 and −65 dB was observed mainly at depths between 20 and 200 m along each transect. In the near ice shelf zone, the SSL was broadly distributed between 50 and 200 m, showing a range of S_v of −80 to −67 dB (Fig. 4a). The SSL in the coastal polynya zone with S_v between −75 and −65 dB was located at a relatively shallower depth of 30–150 m (Fig. 4b). On the other hand, in the pack ice zone region, the SSL was located between 50 and 200 m, except at St. 24 to St. 25, and exhibited relatively weak scattering signals compared to the other two regions, showing a range of S_v of −90 to −75 dB (Fig. 4c). Mesozooplankton, which comprised three copepods (*Rhincalanus gigas*, *Calanoides acutus*, and *Metridia gerlachei*) and ice krill, followed a distribution in relation to environmental features in the Amundsen Sea (Lee et al., 2013; La et al., 2015; Wilson et al., 2015). The acoustic scattering from an individual organism can be expressed as a backscattering cross-section (σ_{bs}, m^2), and as target strength (TS = 10 log$_{10}$(σ_{bs}), dB re 1 m^2). This quantity is fundamental in estimating the number of targets from S_V measurement. Currently, the most common method to estimate copepod and euphausiid σ_{bs} is a distorted-wave Born approximation (DWBA) model (Stanton et al., 1998) and stochastic DWBA (SDWBA) (Demer and Conti, 2005). We used the SDWBA model to estimate euphausiid σ_{bs} at 120 kHz in 0.5 mm length bins between 7 to 37 mm from La et al. (2015). In the SDWBA parameterization, the density and sound-speed contrast (*g* and *h*) values used with 1.0357 and 1.0279 (Foote, 1990), respectively. The swimming orientation angle (θ) was *N* (average standard ± deviation: –8, 9) (La et al., 2015). A ice krill (–75.69 dB) of mean length 24.5 mm, as modeled here, is likely a 10^2-fold stronger acoustic target than a *Neocalanus* sp. copepod of 8 mm (–96.04 dB) body length (Matsukura et al., 2009). S_v from the *Rhincalanus gigas*, *Calanoides acutus*, and *Metridia gerlachei* are weaker than that from *Neocalanus sp.* because of the low TS related to the small body length (Boysen-Ennen et al., 1991). Thus, the most acoustic backscatter in the SSL could be contributed by ice krill.

The main depth of SSL was affected by MLD representing the clear regional differences (Fig. 5). The MLD in the pack ice zone and the coastal polynya zone were generally distributed between 11–21 m and 14–26 m, respectively. The MLD of the water column in the near ice shelf zone was distributed deeper, and ranged between 73 and 89 m. The mean temperature in the mixed layer ranged from −0.49 to −0.01 °C in the coastal polynya zone, −0.59 to −0.55 °C in the near ice shelf zone, and −1.56 to −1.13 °C in the pack ice zone. Because the surface was covered by ice, the relative temperature in the pack ice zone was observed to be colder than in the near ice shelf zone and the coastal polynya zone.

Salinity was largely determined by the melt from sea ice, resulting in regional differences (Fig. 5a). In particular, the coastal polynya zone displayed a halocline layer between the surface to a depth of 30 m. The salinity dropped downed to 33.57–33.69 psμ in the mixed layer (from the surface to MLD), affected by the fresh water from melting sea ice in the pack ice zone (Honjo et al., 2010). Both the coastal polynya zone and the pack ice zone maintained an almost certain salinity under the mixed layer. The water columns near the near ice shelf zone were well mixed between 0 and 200 m, where salinity ranged from 33.91 to 33.93 psμ; a relatively high salinity in the mixed layer compared to the other areas due to the mixing of water masses (Petty et al., 2014).

A distinct characteristic of the vertical distribution of Chl *a* was the subsurface chlorophyll maximum (SCM) and Chl *a* concentration (Fig. 5b). In the coastal polynya zone, Chl *a* levels ranged from 9.64 to 13.55 μg L^{-1}. This was an order of magnitude greater than the concentrations at the other transects, which were 2.79–3.90 μg L^{-1} and 1.66–2.31 μg L^{-1} in the pack ice zone and the near ice shelf zone, respectively. Chl a concentration in the pack ice zone region was broadly exhibited from the surface to 100 m. All maximum levels of Chl a concentration were observed at the surface level. Chl *a* concentration in the near ice shelf zone was lower than that in the other regions.

3.3. Relationship of sound-scattering layer and environmental condition

Diel vertical migration (DVM) can influence the vertical distribution of WMD and S_v variability. The WMD and mean S_v of the SSL are used to indicate the main habitat depths of marine organisms and their relative abundance, with high horizontal and vertical resolution,

Table 3
Results of PERMANOVA based on Euclidean distance matrices derived from log-transformed environmental variables among (F) and between (pair-wise tests) habitats. IS: the near ice shelf zone, CP: the coastal polynya zone, PI: the pack ice zone.

	df	MS	F	*P*
PERMANOVA among habitats				
Habitats	2	118.81	15.017	.001
Residual	54	7.9115		
Total	56			

	df	t	*P*
Pair-wise tests			
PI and IS	34	5.90	0.001
PI and CP	40	4.22	0.001
IS and CP	34	1.9	0.005

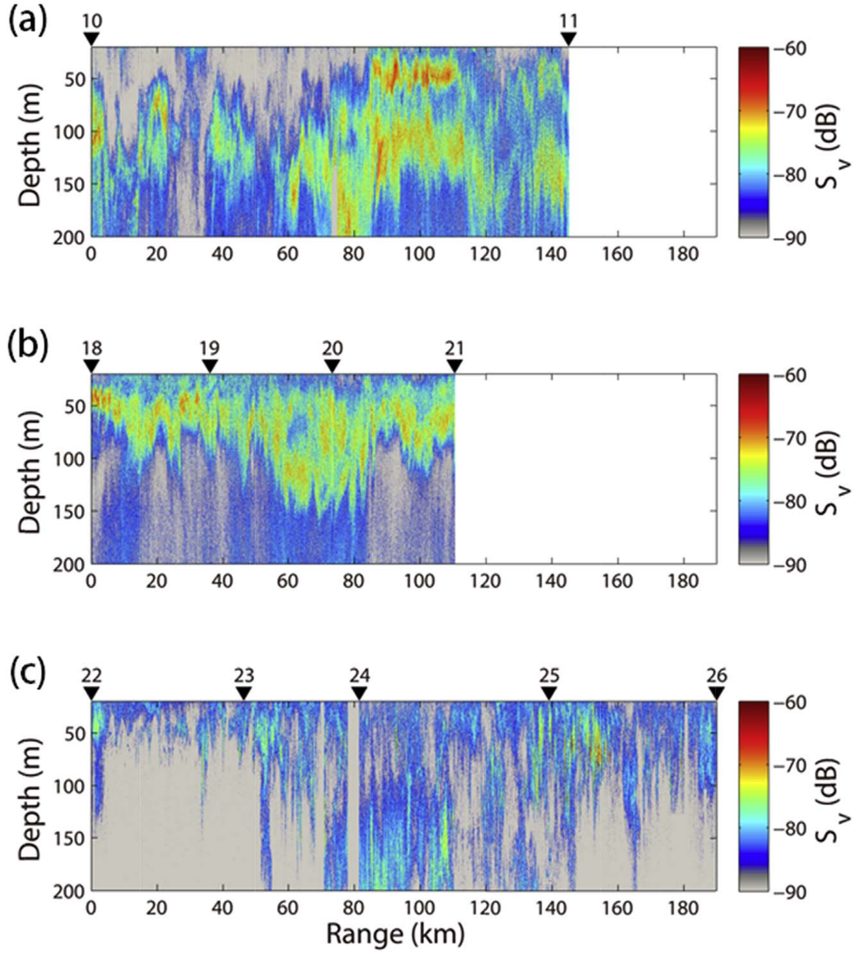

Fig. 4. Echograms for the top 200 m of the water column in the acoustic transect (T1-T3) at 120 kHz, from different geographic resigns in the near ice shelf zone (a), the coastal polynya zone (b), and the pack ice zone (c). Lower threshold is −90 dB.

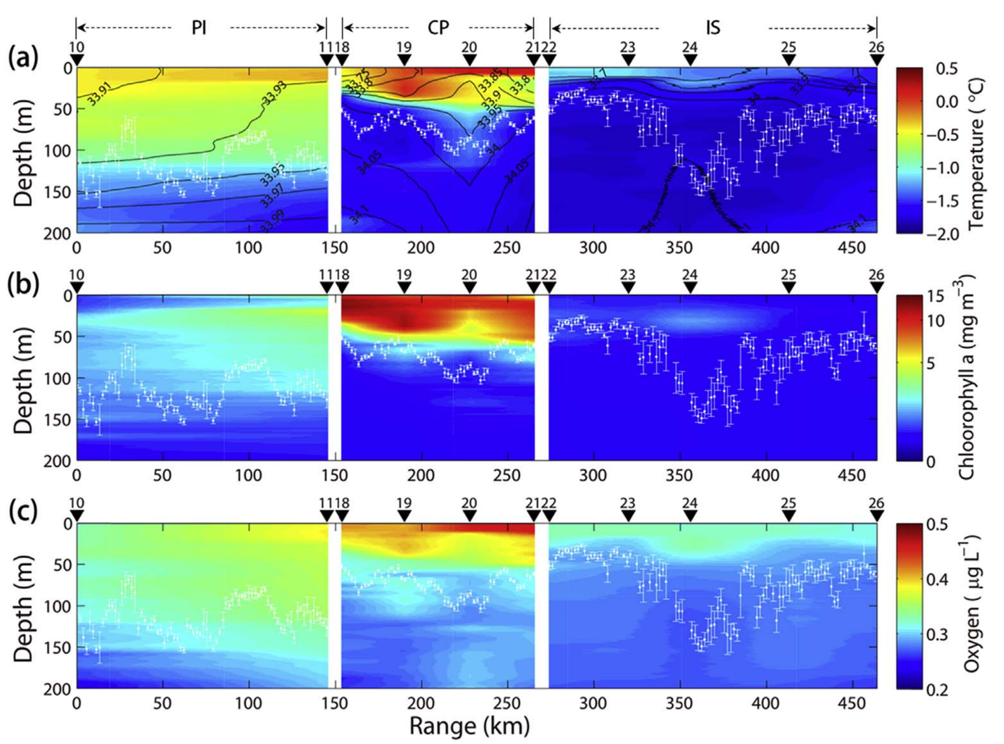

Fig. 5. Environmental properties and pattern of behavior. Mean and standard deviation of weighted mean depth WMD (m, white point and errorbar) along the transect (km) overlaid onto vertical section of temperature (a), chlorophyll *a* (b), and dissolved oxygen (c). Black line in (a) represents salinity (psu) contour. IS: the near ice shelf zone, CP: the coastal polynya zone, PI: the pack ice zone.

Table 4
Weighted mean depth (WMD, m) and mean volume backscattering strength (S_v, dB re 1 m^{-1}) of scattering layer in the Amundsen Sea coastal polynya. IS: the near ice shelf zone, CP: the coastal polynya zone, PI: the pack ice zone.

Station	Region	Mean WMD (SD)	Mean S_v (SD)	MLD (m)	Day/night
10	IS	116.77 (7.81)	−78.71 (0.30)	89	D/N
11	IS	125.88 (6.60)	−80.68 (1.26)	73	D
18	CP	59.60 (7.04)	−75.11 (1.21)	15	D/N
19	CP	63.61 (4.49)	−77.27 (0.95)	22	N
20	CP	84.29 (3.15)	−75.85 (0.50)	26	D
21	CP	65.15 (8.21)	−76.91 (0.71)	20	D
22	PI	57.07 (9.03)	−82.65 (1.53)	14	N
23	PI	47.60 (6.57)	−80.73 (1.73)	11	D
24	PI	126.32 (8.54)	−82.76 (0.28)	17	D
25	PI	59.36 (9.56)	−80.03 (3.76)	12	D
26	PI	52.12 (5.08)	−84.29 (1.65)	21	N

*The day data represent acoustic transects and stations between 00:00 and 18:00 UTC.

respectively. The acoustic transects were undertaken during periods of day or/and night. However, the mean S_v and WMD of each echogram did not show clear differences between day and night (Mann-Whitney *U* test, $p < .05$, Table 4). This is similar result to previous researches in the Amundsen Sea (La et al., 2015; Wilson et al., 2015). Thus, the result indicates that differences in WMD between day and night are not likely to be due to diel vertical behavior of zooplankton.

The WMD of the SSL was calculated at each station to compare regional differences in the main habitat depth of zooplankton (Fig. 6a). The WMD in the near ice shelf zone region was deeper than in the coastal polynya zone and the pack ice zone regions. The deepest depth of WMD was 126.2 m in the near ice shelf zone, which was approximately two times greater than the deepest depths of the other two regions (the coastal polynya zone, 69.5 m; the pack ice zone, 61.4 m), except at St. 24. The WMD was distributed below the MLD varying from 47.6 to 126.3 m at each station, exhibiting a strong linear relationship with the MLD (WMD = MLD × 0.8835 + 45.12, Fig. 6b). Zooplankton abundance collected by the Multiple Opening/Closing Net and Environmental Sensing System (MOCNESS) was low above the MLD, with the subsurface maximum abundance below the MLD in the Amundsen Sea coastal polynya (Wilson et al., 2015). The MLD could be a significant factor controlling the habitat depth of zooplankton, as the water column structure and temperature has a major influence on zooplankton biology (Iguchi and Ikeda, 2004).

Notably, Pearson correlation analysis also determined that the WMDs of the SSL were positively correlated with the MLD (r = 0.69, $p < .05$). On the other hand, both the SSL and WMD near St. 24 represented a slightly different pattern than those around the pack ice zone (Figs. 5 and 6). We assume that this could be affected by different marine organisms such as the Antarctic silverfish, Pleuragramma antarcticum. Silverfish, a key link between zooplankton and top predators (Smith et al., 2007; O'Driscoll et al., 2011), is the most abundant species in the coastal shelf of the Southern Ocean (Hubold, 1985). Ice krill are often observed up to 200 m depth (Everson, 1987; Pakhomov et al., 1998; Guglielmo et al., 2009; La et al., 2015), while adult silverfish tend to distribute a deeper depth ranging from 100 to 400 m. This could imply that the vertical habitats of ice krill and silverfish could be separately responding to the different patterns associated with water column properties.

Phytoplankton is generally considered as a primary food source of zooplankton, influencing zooplankton growth and development rates (Daly, 1990; Whitehouse et al., 2009). In the Amundsen Sea, the phytoplankton bloom is regularly observed in January, and the peak of phytoplankton bloom is presented in the center of the coastal polynya (Arrigo et al., 2012). Light is an important factor that regulates phytoplankton biomass in the high-latitude coastal polynyas of the Southern Ocean (Alderkamp et al., 2015; La and Park, 2016). Light availability in the Amundsen Sea is spatially variable (Arrigo et al., 2012), depending on the existence of sea ice and the ice shelf. Sea ice concentration can limit the penetration of solar radiation into the ocean by 15–90% (Anderson et al., 1998), and the fresh melting water from ice-shelf can destabilize the water column, increasing the mixed layer depth and decreasing light availability (Alderkamp et al., 2012). Lee et al. (2013) found the abundance of ice krill to be positively correlated with Chl *a* in the Amundsen Sea during summer. In this study, a similar association was observed in the mean S_v, implying the abundance of zooplankton showed a strong positive correlation with the maximum Chl *a* in the subsurface chlorophyll maximum ($r = 0.87$, $p < .01$). A high mean S_v was observed in the coastal polynya zone, which was approximately 4 and 8 dB higher than in the pack ice zone and the near ice shelf zone, respectively (Table 4). Considering that the mean length of ice krill observed here was 21.2 mm (La et al., 2015), the biomass in the coastal polynya zone was about 60.2–90.3% higher than those of the pack ice zone and the near ice shelf zone. This indicates that the different phytoplankton biomass of the three habitats may affect the zooplankton biomass around the pack ice zone, the coastal polynya zone, and the near ice shelf zone.

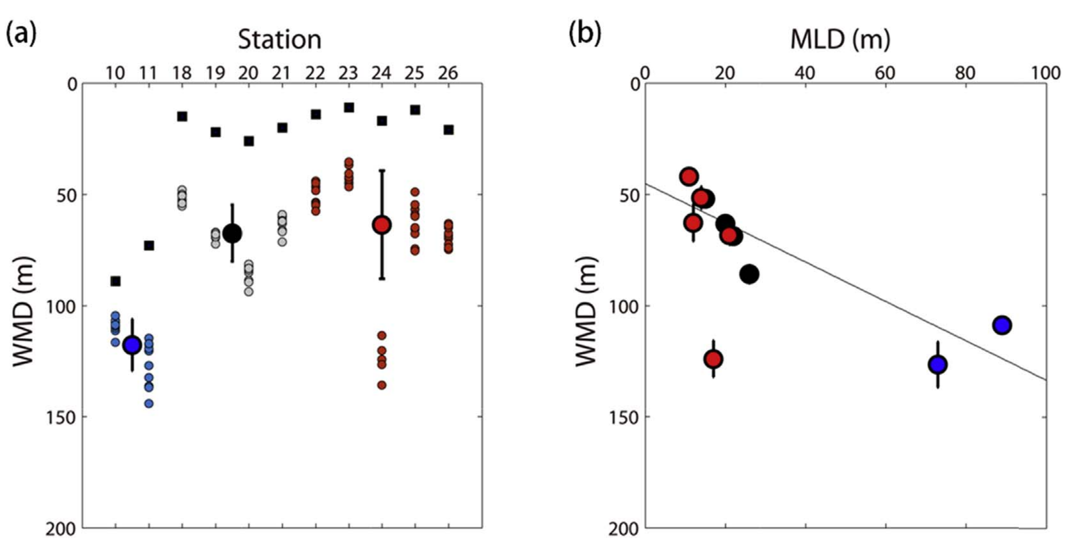

Fig. 6. (a) Spatial variation of the WMD of scattering layers within the Amundsen Sea, means (blue, black, and red circle with error bar in the IS, CP, and PI, respectively) for acoustic transects at each station, black square is the MLD. (b) Relationship between MLD and WMD of scattering layer (WMD = MLD × 0.8835 + 45.12, r = 0.69, p < .05). Blue, black, and red circle with error bar represent the near ice shelf zone (IS), the coastal polynya zone (CP), and the pack ice zone (PI). (For interpretation of the references to colour in this figure legend, the reader is referred to the Web version of this article.)

4. Conclusions

We present the regional differences in the SSL, representing the zooplankton distribution in the Amundsen Sea. High-latitude coastal water in the Southern Ocean is an important habitat for the polar ecosystem; however, relatively little is known about zooplankton distribution due to the harsh sea ice conditions. The SSL was mainly distributed under the MLD, while exhibiting strong positive correlation with it. In the ice shelf of the Antarctic Ocean, freshwater input from melting sea-ice or glaciers is recognized as the principal factor in stabilizing the upper water column by causing variability in the MLD during summer. The MLD affects light intensity and nutrient availability for phytoplankton, which in turn affects phytoplankton production at the base of the pelagic food web. This suggests that the MLD can be an essential environmental factor, which could control the habitat depth of zooplankton in the ice-covered region in the Southern Ocean.

Acknowledgments

This work was supported by grants from KOPRI (PP17060) and the National Institute of Fisheries Science (R2018029).

References

Alderkamp, A.C., van Dijken, G.L., Lowry, K.E., Connelly, T.L., Lagerström, M., Sherrell, R.M., Haskins, C., Rogalsky, E., Schofiled, O., Stammerjohn, S.E., 2015. Fe availability drives phytoplankton photosynthesis rates during spring bloom in the Amundsen Sea Polynya. Antarctica. Elem Sci Anth. 3, 000043.
Alderkamp, A.C., Mills, M.M., Van Dijken, G.L., Laan, P., Thuyroczy, C.E., Gerringa, L.J.A., de Baar, H.J.W., Payne, C.D., Visser, R.J.W., Buma, A.G.J., Arrigo, K.R., 2012. Iron from melting glaciers fuels phytoplankton blooms in the Amundsen Sea (Southern Ocean): phytoplankton characteristics and productivity. Deep Sea Res 71, 32–48.
Ambler, J.W., Miller, C.B., 1987. Vertical habitat-partitioning by copepodites and adults of subtropical oceanic copepods. Mar. Biol. 94, 561–577.
Anderson, L.G., Olsson, K., Jones, E.P., Chierici, M., Fransson, A., 1998. Anthropogenic carbon dioxide in the Arctic Ocean: inventory and sinks. J Geophys Res Oceans 103, 27707–27716.
Anderson, M.J., Gorley, R.N., Clarke, K.R., 2008. PERMANOVA+ for PRIMER Guide to Software and Statistical Methods. PRIMER-E Ltd., Plymouth.
Arrigo, K.R., Lowry, K.E., van Dijken, G.L., 2012. Annual changes in sea ice and phytoplankton in polynyas of the Amundsen Sea, Antarctica. Deep Sea Res 71, 5–15.
Atkinson, A., 1998. Life cycle strategies of epipelagic copepods in the Southern Ocean. J. Mar. Syst. 15, 289–311.
Bathmann, U., Priddle, J., Treguer, P., Lucas, M.I., Parslow, J., Hall, J., 2000. Plankton ecology and biogeochemistry in the Southern Ocean: a first review of Southern Ocean JGOFS. In: In: Hanson, R., Ducklow, H.W., Field, J.G. (Eds.), The Changing Ocean Carbon Cycle: a Mid-term Synthesis of the JGOFS, vol. 5. Cambridge University Press, UK, pp. 300–337.
Brierley, A.S., Saunders, R.A., Bone, D.G., Murphy, E.J., Enderlein, P., Conti, S.G., Demer, D.A., 2006. Use of moored acoustic instruments to measure short-term variability in abundance of Antarctic krill. Limnol Oceanogr. Meth. 4, 18–29.
Boysen-Ennen, E., Hagen, W., Hubold, G., Piatkowski, U., 1991. Zooplankton biomass in the ice-covered Weddell Sea, Antarctica. Mar. Biol. 111 (2), 227–235.
CCAMLR, 2010. Report of the Fifth Meeting of the Subgroup on Acoustic Survey and Analysis Methods. SC-CCAMLR-XXIX/6.
Clarke, K.R., Gorley, R.N., 2006. PRIMER 6 User Manual/Turorial. PRIMER-E Ltd., Plymouth.
Cornet, C., Gili, J.M., 1993. Vertical distribution and daily migrations of hyperiid amphipods in the northern Benguela in relation to water column stratification. Deep Sea Res 40, 2295–2306.
Daly, K.L., 1990. Overwintering development, growth, and feeding of larval Euphausia superba in the Antarctic marginal ice zone. Limnol. Oceanogr. 35, 1564–1576.
Demer, D.A., Conti, S.G., 2005. New target-strength model indicates more krill in the Southern Ocean. ICES J. Mar. Sci. 62, 25–32.
Diehl, S., Berger, S.A., Ptacnik, R., Wild, A., 2002. Phytoplankton, light, and nutrients in a gradient of mixing depths: weld experiments. Ecology 83, 399–411.
Everson, I., 1987. Life in a cold environment. Antarct. Sci. 69–137.
Fielding, S., Watkins, J.L., Collins, M.A., Enderlein, P., Venables, H.J., 2012. Acoustic determination of the distribution of fish and krill across the Scotia Sea in spring 2006, summer 2008 and autumn 2009. Deep Sea Res. Part II Top. Stud. Oceanogr. 59, 173–188.
Foote, K.G., Knudsen, H.P., Vestnes, G., MacLennan, D.N., Simmonds, E.J., 1987. ICES Co-operative Research Report. Calibration of Acoustic Instruments for Fish Density Estimation: a Practical Guide, vol. 144. pp. 69.
Foote, K.G., 1990. Speed of sound in Euphausia superba. J. Acoust. Soc. Am. 87, 1405–1408.
Guglielmo, L., Donato, P., Zagami, G., Granata, A., 2009. Spatio-temporal distribution and abundance of Euphausia crystallorophias in Terra Nova Bay (Ross Sea, Antarctica) during austral summer. Polar Biol. 32, 347–367.
Hamner, W.M., Hamner, P.P., Strand, S.W., Gilmer, R.W., 1983. Behavior of Antarctic krill Euphausia superba: chemoreception, feeding, schooling, and molting. Science [Washington D.C.] 220, 433–435.
Honjo, S., Krishfield, R.A., Eglinton, T.I., Manganini, S.J., Kemp, J.N., Doherty, K., Takizawa, T., 2010. Biological pump processes in the cryopelagic and hemipelagic Arctic Ocean: Canada Basin and Chukchi Rise. Prog. Oceanogr. 85, 137–170.
Hubold, G., 1985. Stomach contents of the Antarctic silverfish Pleuragramma antarcticum from the southern and eastern Weddell Sea (Antarctica). Polar Biol. 5, 43–48.
Iguchi, N., Ikeda, T., 2004. Effects of temperature on metabolism, growth and growth efficiency of Thysanoessa longipes (Crustacea: euphausiacea) in the Japan Sea. J. Plankton Res. 27, 1–10.
Jacobs, S.S., Jenkins, A., Giulivi, C.F., Dutrieux, P., 2011. Stronger ocean circulation and increased melting under Pine Island Glacier ice shelf. Nat. Geosci. 4, 519–523.
Jenkins, A., Dutrieux, P., Jacobs, S.S., McPhail, S.D., Perrett, J.R., Webb, A.T., White, D., 2010. Observations beneath Pine Island glacier in West Antarctica and implications for its retreat. Nat. Geosci. 3, 468–472.
Jiang, Y., Yang, E.J., Kim, S.Y., Kim, Y.N., Lee, S., 2014. Spatial patterns in pelagic ciliate community responses to various habitats in the Amundsen Sea (Antarctica). Prog. Oceanogr. 128, 49–59.
La, H.S., Lee, H., Fielding, S., Kang, D., Ha, H.K., Atkinson, A., Park, J., Siegel, V., Lee, S.H., Shin, H., 2015. High density of ice krill (Euphausia crystallorophias) in the Amundsen sea coastal polynya, Antarctica. Deep Sea Res. Part I 95, 75–84.
La, H.S., Park, K., 2016. The evident role of clouds on phytoplankton abundance in antarctic coastal polynyas. Terr. Atmos. Ocean Sci. 27, 293–301.
Lee, D.B., Choi, K.H., Ha, H.K., Yang, E.J., Lee, S.H., Lee, S.H., Shin, H.C., 2013. Mesozooplankton distribution patterns and grazing impacts of copepods and Euphausia crystallorophias in the Amundsen Sea, West Antarctica, during austral summer. Polar Biol. 36, 1215–1230.
Matsukura, R., Yasuma, H., Murase, H., Yonezaki, S., Funamoto, T., Honda, S., Miyashita, K., 2009. Measurements of density contrast and sound-speed contrast for target strength estimation of Neocalanus copepods (Neocalanus cristatus and Neocalanus plumchrus) in the North Pacific Ocean. Fish. Sci. 75, 1377–1387.
O'Driscoll, R.L., Macaulay, G.J., Gauthier, S., Pinkerton, M., Hanchet, S., 2011. Distribution, abundance and acoustic properties of Antarctic silverfish (Pleuragramma antarcticum) in the Ross Sea. Deep Sea Res. Part II Top. Stud. Oceanogr. 58, 181–195.
Petty, A.A., Holland, P.R., Feltham, D.L., 2014. Sea ice and the ocean mixed layer over the Antarctic shelf seas. Cryosphere 8, 761–783.
Pakhomov, E.A., Perissinotto, R., Froneman, P.W., 1998. Abundance and trophodynamics of Euphausia crystallorophias in the shelf region of the Lazarev Sea during austral spring and summer. J. Mar. Syst. 17, 313–324.
Pinkerton, M., Smith, A.N., Raymond, B., Hosie, G.W., Sharp, B., Leathwick, J.R., Bradford-Grieve, J.M., 2010. Spatial and seasonal distribution of adult Oithona similis in the Southern Ocean: predictions using boosted regression trees. Deep Sea Res. Oceanogr. Res. Paper 57, 469–485.
Ross, R.M., Quetin, L.B., Martinson, D.G., Iannuzzi, R.A., Stammerjohn, S.E., Smith, R.C., 2008. Palmer LTER: patterns of distribution of five dominant zooplankton species in the epipelagic zone west of the Antarctic Peninsula, 1993–2004. Deep Sea Res. Part II Top. Stud. Oceanogr. 55, 2086–2105.
Saito, H., Hattori, H., 1997. Diel vertical migration and feeding rhythm of copepods in a shallow, food-abundant embayment. Plank. Benth. Res. 44, 13–29.
Schneider, N., Müller, P., 1990. The meridional and seasonal structures of the mixed-layer depth and its diurnal amplitude observed during the Hawaii-to-Tahiti Shuttle experiment. J. Phys. Oceanogr. 20, 1395–1404.
Schneider, D.P., Deser, C., Okumura, Y., 2012. An assessment and interpretation of the observed warming of West Antarctica in the austral spring. Clim. Dyn. 38, 323–347.
Sebastian, P., Stibor, H., Berger, S., Diehl, S., 2012. Effects of water temperature and mixed layer depth on zooplankton body size. Mar. Biol. 159, 2431–2440.
Smith, J.A., Hillenbrand, C.D., Kuhn, G., Larter, R.D., Graham, A.G., Ehrmann, W., Moreton, S.G., Forwick, M., 2011. Deglacial history of the West Antarctic ice sheet in the western Amundsen Sea embayment. Quat. Sci. Rev. 30, 488–505.
Smith, W.O., Ainley, D.G., Cattaneo-Vietti, R., 2007. Trophic interactions within the Ross Sea continental shelf ecosystem. Philos. Trans. R. Soc. London Ser. B 362, 95–111.
Solberg, I., Røstad, A., Kaartvedt, S., 2015. Ecology of overwintering sprat (Sprattus sprattus). Prog. Oceanogr. 138, 116–135.
Stanton, T.K., Chu, D., Wiebe, P.H., 1998. Sound scattering by several zooplankton groups. II. Scattering models. J. Acoust. Soc. Am. 103, 236–253.
Swadling, K.M., Kawaguchi, S., Hosie, G.W., 2010. Antarctic mesozooplankton community structure during BROKE-West (30 E–80 E), January–February 2006. Deep Sea Res. Part II Top. Stud. Oceanogr. 57, 887–904.
Turner, J., Comiso, J.C., Marshall, G.J., Lachlan-Cope, T.A., Bracegirdle, T., Maksym, T., Meredith, M.P., Wang, Z., Orr, A., 2009. Non-annular atmospheric circulation change induced by stratospheric ozone depletion and its role in the recent increase of Antarctic sea ice extent. Geophys. Res. Lett. 36.
Watkins, J.L., Brierley, A.S., 1996. A post-processing technique to remove background noise from echo integration data. ICES J. Mar. Sci. 53, 339–344.
Whitehouse, M.J., Atkinson, A., Ward, P., Korb, R.E., Rothery, P., Fielding, S., 2009. Role of krill versus bottom-up factors in controlling phytoplankton biomass in the northern Antarctic waters of South Georgia. Mar. Ecol. Progr 393, 69–82.
Wilson, S.E., Swalethorp, R., Kjellerup, S., Wolverton, M.A., Ducklow, H.W., Yager, P.L., 2015. Meso-and macro-zooplankton community structure of the Amundsen Sea Polynya, Antarctica (summer 2010–2011). Elementa 3.